Hindawi
International Journal of Agronomy
Volume 2023, Article ID 5686484, 9 pages
https://doi.org/10.1155/2023/5686484

Research Article

Molecular Cloning, Subcellular Localization, and Abiotic Stress Induction Analysis of a Polyamine Oxidase Gene from *Oryza sativa*

Ishita Samanta, Shweta Chaturvedi, Pamela Chanda Roy, and Gopal Chowdhary

Plant Molecular Biology Laboratory, School of Biotechnology, KIIT, Bhubaneswar 751024, Odisha, India

Correspondence should be addressed to Gopal Chowdhary; gopal.chowdhary16@gmail.com

Received 15 August 2022; Revised 4 November 2022; Accepted 20 March 2023; Published 17 April 2023

Academic Editor: Nasim Ahmad Yasin

Abiotic stress is a major bottleneck for crop productivity. To counter abiotic stresses, plants have developed several strategies, and the accumulation of polyamine (PA) serving as an osmolyte is one of them. The cellular pool of PAs is primarily regulated by polyamine oxidases (PAOs) either by terminal catabolism or by back conversion (BC) of polyamines. The role of PAO in abiotic stress tolerance has also been reported. Polyamine oxidases are primarily localized in the cytosol, cell wall, and apoplastic regions; however, lately, their peroxisomal localization has also been demonstrated. In this study, we reported the detection of polyamine oxidase isoform 3 from *Oryza sativa* (OsPAO3) in peroxisome as early as 12 h post-transformation under *in vitro* conditions using fluorescent microscopy. The gene was also found to be significantly upregulated by salinity, dehydration, cold, and heat stress. We have also demonstrated that the expression of *OsPAO3* gene was mediated by a second messenger, calcium. The upregulation of *OsPAO3* by salinity, dehydration, cold, and heat stresses suggests that it could be a suitable candidate for providing tolerance to plants against abiotic stress combination or stress matrix, which is a common feature in agricultural field conditions. Furthermore, the data provided here would be valuable in understanding the abiotic stress-mediated signal transduction network of PAOs.

1. Introduction

Being sessile in nature, plants are not able to escape from the adversaries of the various abiotic stresses. To withstand these harsh conditions, plants have developed sophisticated mechanisms of perception, signaling, and counter-response. One such response is the accumulation of polyamines (PA), which are small aliphatic amines present in almost all organisms starting from prokaryotes to eukaryotes [1]. They can be diamine (putrescine), triamine (spermidine), or tetramine (spermine). Usually, these three types of PAs are predicted to have similar biological functions; however, their signatures may differ [1–3]. In plants, PAs have been suggested to be involved in a wide range of functions, from embryogenesis to senescence, including stress tolerance [1, 4].

The cellular PA levels primarily depend upon two types of amine oxidases; copper-containing amine oxidases (CuAOs) and FAD-dependent polyamine oxidases (PAO). The role of PAOs has been implicated in both catabolism and biosynthesis of PAs, referred to as terminal catabolism (TC) and back conversion (BC) type PAO, respectively [1]. The TC-type PAO catalyzes the oxidative deamination of PAs. The end product of this conversion is 4-aminobutanal and N-(3-aminopropyl)-4-aminobutanal, respectively, for spermidine (Spd) and spermine (Spm), along with concomitant production of 1,3-diaminopropane and hydrogen peroxide (H_2O_2) [5–7]. The BC-type PAO leads to the conversion of tetramine (Spm and thermospermine) to triamine (Spd) and triamine to diamine (putrescine) [5–8].

Multiple isoforms of PAOs have been reported in various plant species. The model plant *Arabidopsis thaliana* and *Oryza sativa* have been reported to contain five and seven PAO isoforms, respectively [3, 4]. They have been found to be localized in the cytosol, cell wall, apoplastic region, and peroxisomes [3, 4]. The role of PAOs has also been

implicated in abiotic stress tolerance [9–12]. A common after-effect of all the abiotic stresses is an increase in the cellular concentration of reactive oxygen species (ROS), and in plant cells, peroxisome in addition to chloroplast and mitochondria acts as one of the nodal centers for ROS homeostasis [13]. Owing to the significance of peroxisomes and PAOs in abiotic stress tolerance, the peroxisomal isoforms of PAOs are of much significance. The model plant *A. thaliana* and *O. sativa* contain three such isoforms each, namely, AtPAO2, AtPAO3, and AtPAO4 [3, 6, 14] and OsPAO3, OsPAO4, and OsPAO5 [4].

Furthermore, in abiotic stress signaling, after the perception of the signal, the second messenger plays a critical role in further transducing the message to the downstream components. Normally, calcium has been proposed as a potential second messenger in the majority of abiotic stress signal transduction pathways [15, 16]. The indirect involvement of calcium in PAO-mediated signaling has also been observed [17, 18].

The peroxisomal localization of certain PAOs and their involvement in abiotic stress tolerance have already been documented. Peroxisomes being a nodal center for ROS homeostasis play a significant role in abiotic stress tolerance. A BC-type PAO leads to back conversion of PAs, thereby increasing the cellular concentration of PAs and helping in abiotic stress acclimation. However, it would be interesting to understand at what stage (either early or late) of stress acclimation PAOs play a role, and how their signaling is mediated. In order to understand these, we have used OsPAO3, a BC-type peroxisomal PAO from *O. sativa*. In this study, we studied the time-dependent subcellular localization combined with detailed expression analysis of *OsPAO3* to investigate the involvement of PAO in the early or late stage of stress acclimation. Furthermore, an attempt was made to investigate the underlying second messenger in order to speculate the probable mode of abiotic stress-mediated PAO signaling.

2. Materials and Methods

2.1. Plant Material and Stress Treatment. For all experiments, 11-day-old *O. sativa* IR 64 (Indica rice variety) seedlings were used. The seeds of *O. sativa* were obtained from the National Rice Research Institute, Cuttack, India. This is an abiotic stress-sensitive variety. The seedlings were grown in a plant growth chamber maintained at $28 \pm 2^{\circ}$C, 60% humidity, and a light/dark cycle of 16/8 h. The abiotic stresses were induced by treatment with 200 mM sodium chloride (saline stress), 15% PEG 6000 (dehydration stress), $4 \pm 2^{\circ}$C (cold stress), and $45 \pm 2^{\circ}$C (heat stress). Treatments were given for 0.5, 1, 2, 4, 8, 16, and 24 h. The untreated seedlings served as a control and were used for the calculation of the relative transcript level of *OsPAO3*. All the experiments have been performed a minimum of three times.

2.2. RNA Extraction and Cloning of OsPAO3. Extraction of RNA was conducted using RNeasy plant mini kit from Qiagen as per the manufacturer's protocol, with the modification of inclusion of in-column DNase digestion step (RNase free DNase set, Qiagen, 79254). The extracted RNA was checked for its quantity and quality using a microvolume spectrophotometer (Thermo Fisher Scientific) and agarose gel electrophoresis (Bio-Rad), respectively.

The extracted RNA was converted to cDNA using Revert Aid First Strand cDNA Synthesis Kit (Thermo Fisher Scientific) as per the manufacturer's manual. The obtained cDNA was used for polymerase chain reaction amplification using the primers: forward AATTGCGGCCGCGATGGC GAACAACAGTTCATATGGTG and reverse TATGCC GCGGTCATCACAGCCGGGAGATGAGCAGTG, using HiFidelity polymerase (Qiagen), with PCR cycle of denaturation at 94°C for 20 s, annealing at 60°C for 30 s, and extension at 72°C for 90 s. The obtained PCR product was checked for amplification using agarose gel electrophoresis followed by digestion using NotI and SacII restriction enzymes. The digested product was resolved on an agarose gel followed by gel purification using the GenJET gel extraction kit (Thermo Fisher Scientific). The digested product was cloned in a pCAT plant expression vector under the control of a double 35 S cauliflower mosaic virus (CaMV) promoter [19]. The insert was verified using an automated DNA sequencing. No mutations were detected.

2.3. Subcellular Localization of OsPAO3. The gene of interest (*OsPAO3*) was cloned as a fusion product of enhanced yellow fluorescent protein (EYFP). DsRed-SKL was used as a peroxisomal marker to decipher the identity of the organelle [20]. In the case of single transformation experiments, pCAT plasmid containing EYFP-*OsPAO3* was coated with gold particles, while in the case of double transformation experiments, both the pCAT plasmid containing EYFP-*OsPAO3* and peroxisomal marker (Ds-Red-SKL) were coated with gold particles and bombarded to onion epidermal cells [21]. The onion slices were placed on a wet blotting paper in Petri dishes and stored at room temperature in the dark for approximately 12 h/18 h/24 h, followed by analysis using fluorescent microscopy. Image capture and analysis were conducted as explained [22].

2.4. Protoplast Isolation. Green tissues from the stem to sheath of about 40–60 *O. sativa* seedlings were cut together into approximately 1 mm strips using a sharp razor blade. The strips were incubated in 0.5 M mannitol for 10 min in the dark, followed by O/N incubation in an enzyme solution containing 1.5% cellulase and 0.75% macerozyme. After the enzymatic digestion, an equal volume of W5 solution (154 mM NaCl, 125 mM $CaCl_2.2H_2O$, 5 mM KCl, and 5 mM Glucose) was added, followed by vigorous shaking for 10 s to detach the protoplasts. Protoplasts were filtered through nylon meshes into 15 mL tubes with 3–5 washes of the strips using the W5 solution. The pellet was collected by centrifugation at 1,500 rpm for 5 min at 4°C in a swinging bucket rotor. The pellet was resuspended in 5 mL of W5 medium and centrifuged again at 1,500 rpm for 5 min at 4°C. The pellet obtained was resuspended in 5 mL of W5 medium and incubated in ice for 1 h. The protoplast concentration was

determined by using a hemocytometer. After incubation in ice for 1 h, the suspension was centrifuged (1,500 rpm, 5 min, 4°C), and the pellet obtained was resuspended in ice-cold MaMg solution (0.5 M Mannitol, 15 mM $MgCl_2.6H_2O$, 0.1% MES). The protoplast obtained was used for various treatments; 200 mM sodium chloride [23, 24], 50 μM calcium ionophore A23187 [25, 26], 2 mM calcium channel blocker verapamil [27], and 2 mM calcium chelator BAPTA (1,2-bis(o-amino phenoxy) ethane-N,N,N′,N′-tetra acetic acid) [26, 28]. The treatments were given for 2 h. After treatment, RNA extraction was performed as described in Section 2.2.

2.5. Real-Time PCR. The total RNA was extracted from stress-treated and control (untreated) seedlings as explained above (Section 2.2), its concentration was determined and equalized, and 1 μg of total RNA was converted to cDNA using a high-capacity cDNA reverse transcription kit (Thermo Fisher Scientific) as per the manufacturer's manual and was further used for quantitative real-time PCR analysis using TaqMan™ Open Array™ Real-Time PCR Master Mix (Thermo Fisher Scientific). The reactions were carried out by multiplexing. The *OsPAO3* was labeled with FAM, and endogenous control eukaryotic elongation factor 1 (*OseEF1*) α was labeled with VIC reporter dye, respectively. The TaqMan probes were custom synthesized by Thermo Fisher Scientific. Thermal cycling conditions were as follows: hold stage of 2 min at 50°C, followed by 10 min at 95°C, 40 cycles of denaturation at 95°C for 15 s, and annealing and extension at 60°C for 1 min. The data were captured during the annealing and extension stage. The relative transcript level or "fold change" (degree of change in expression between the treated sample and untreated sample) was calculated by the ΔΔCT method using the formula, relative transcript level/fold change = $2^{-\Delta\Delta CT}$, where ΔΔCT = ΔCT test sample − ΔCT calibrator sample (ΔCT test sample = CT test − CT reference, ΔCT calibrator = CT calibrator − CT reference; test sample = treated sample, calibrator = untreated sample, and reference = endogenous control) [29]. The data provided represent an average of three biological replicates of independent samples, and the values depicted represent mean ± standard deviation.

3. Results

3.1. Molecular Cloning and Subcellular Localization of OsPAO3. The cDNA of the *O. sativa* was used as a template for PCR-based cloning of *OsPAO3*. The primer sequences and PCR cycle are explained in the materials and method section (Section 2.2). The PCR amplified product was found to be of 1500 bp and was cloned in the pCAT vector under the control of a double 35 S CaMV promoter. The gene was cloned as a C-terminal fusion of EYFP. The sequence of the cloned gene was verified using an automated DNA sequencing. No mutations were detected.

For subcellular localization studies, the biolistic bombardment method was used, in which onion epidermal cells were transformed with plasmid constructs coated on gold particles, which were further examined under a fluorescent microscope after an appropriate incubation time. Under standard conditions, the transformed onion epidermal cells are examined after 18–24 h post-transformation (p.t.). Onion epidermal cells transformed only with EYFP, which served as a negative control, showed uniform cytosolic fluorescence (Figure 1(a)). The OsPAO3 which was expressed as a fusion product of EYFP was observed in small punctuate structures after 12 h and 18–24 h p.t. (Figures 1(b) and 1(c)). The identity of fluorescent punctuate structures was confirmed by double transformation experiments coexpressing peroxisomal marker DsRed-SKL. The double transformation experiments demonstrated the overlapping of both green and red fluorescence from EYFP and peroxisomal marker, respectively (Figures 1(d) and 1(e)), confirming the identity of the punctuate fluorescing organelle to be peroxisome. The finding suggests that the PAO3 from *O. sativa* was detectable in peroxisome as early as 12 h p.t.

3.2. Expression Analysis of OsPAO3. For *OsPAO3* gene expression analysis, the abiotic stress-treated seedlings were used for RNA extraction, followed by cDNA synthesis and real-time PCR. The untreated seedlings were used as a control. The expression data were represented as relative transcript level or "fold change" which essentially means the change in the degree of expression between the treated sample and untreated samples. The details are explained in the materials and methods (Section 2.5).

3.2.1. Salt Stress Analysis. The expression pattern of *OsPAO3* was checked at 0.5, 1, 2, 4, 8, 16, and 24 h of 200 mM sodium chloride treatment. The *OsPAO3* mRNA expression rose to 3.7-fold (meaning 3.7 times higher than that of the untreated condition) at 0.5 h, followed by a drop in the transcript level to 1.7-fold at 1 h. The expression of *OsPAO3* again increased to 12-fold at 2 h followed by a steady decline with time and finally reaching 3.2-fold at 24 h (Figure 2(a)). The peak of transcript accumulation was observed at 2 h of sodium chloride treatment. The transcript level of *OsPAO3* increased at 0.5 h followed by a drop at 1 h, and a second surge (increase) in transcript accumulation suggests that *OsPAO3* expression follows a pulsating pattern.

3.2.2. Cold Stress Analysis. Cold stress was given at 4 ± 2°C for 0.5, 1, 2, 4, 8, 16, and 24 h. At 0.5 h, the expression of *OsPAO3* increased to 2.5-folds followed by a drop in the transcript level of *OsPAO3* at 1 h. The transcript level at 1 h was found to be lesser than at the control level. However, after 1 h, the *OsPAO3* transcript accumulation increased to 1.4-fold at 2 h and then peaked to 3-fold at 4 h. Beyond 4 h of cold treatment, the expression reduced, and a basal level of expression of 1.8–2.0-fold was maintained (Figure 2(a)). The cold stress treatment also showed a pulsating pattern of expression, i.e., expression increased at 0.5 h, followed by a drop, and again increased in transcript accumulation at 4 h.

3.2.3. Drought Stress Analysis. Dehydration stress was given by treating the seedlings with PEG6000, which led to the withdrawal of water. The *OsPAO3* expression increased to a 4.2-fold at 0.5 h, followed by a reduction in the transcript

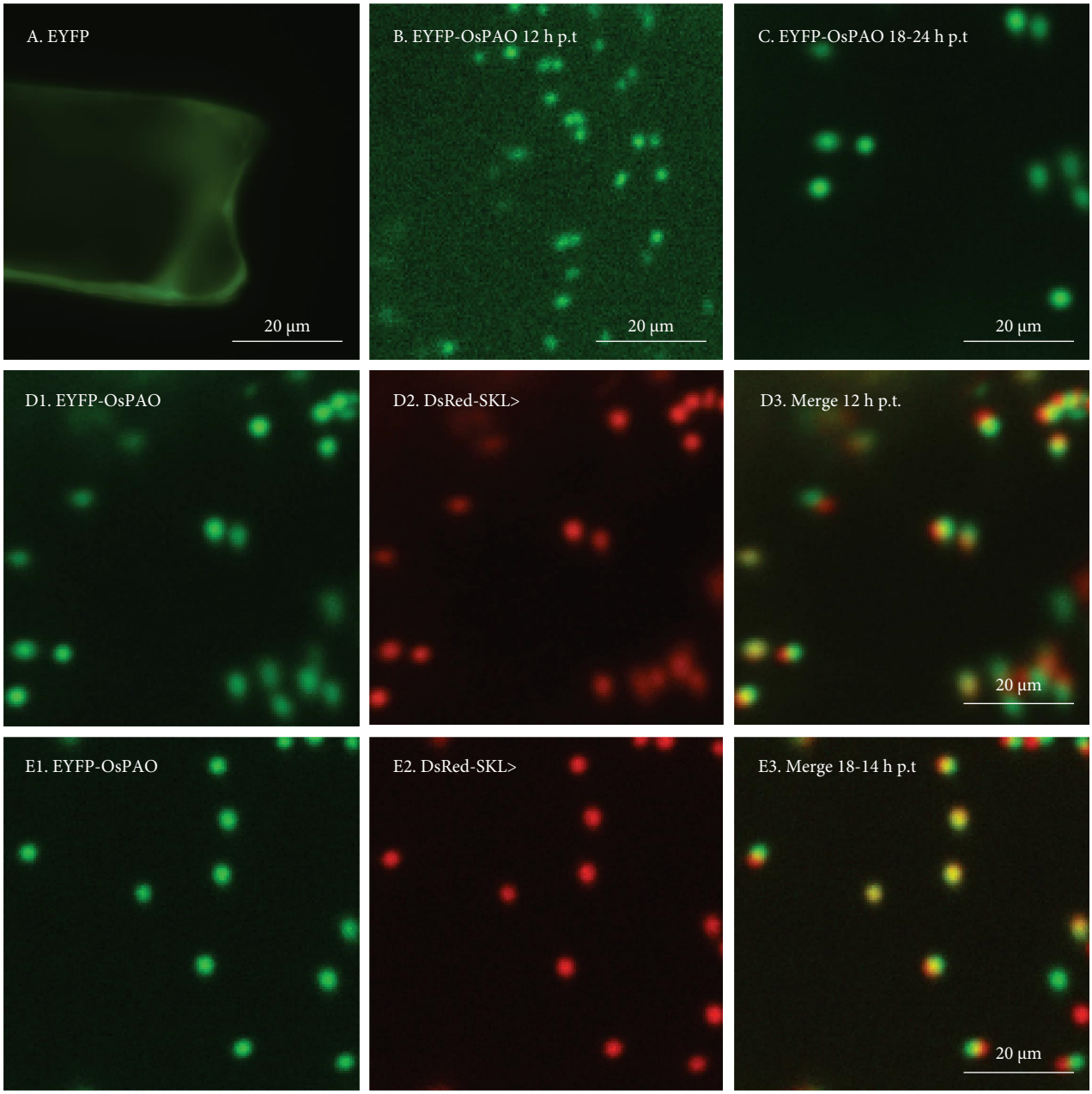

Figure 1: Subcellular localization of OsPAO3. The *OsPAO3* was cloned in the plant transient expression vector pCAT as an EYFP fusion construct. DsRed SKL was used as a peroxisome marker. The plasmids of interest were coated with gold particles followed by biolistic bombardment of onion epidermal cells. The onion epidermal cells were incubated at room temperature followed by analysis using fluorescence microscopy. (a) The cytosolic EYFP fluorescence. (b, c) The EYFP fluorescence localized in punctate structure after 12 and 18 h p.t., which were confirmed to be peroxisomes upon colocalization with peroxisomal marker DsRed-SKL. (d, e) Imaging 12 h and 18–24 h p.t., respectively.

level to 1.5-fold at 1 h. The expression further again increased to 3.6-fold at 2 h, followed by a decrease in transcript accumulation to approximately 2-fold till further time points (Figure 2(a)). The peak of transcript accumulation was observed at 2 h.

In the case of salinity, cold, and dehydration stress, a similarity in the expression pattern was observed. The expression of *OsPAO3* was found to be pulsating in nature, i.e., the expression increased at initial time points (0.5 h), followed by a reduction in the expression, and again a second surge (increase) in expression (2/4 h) was observed.

3.2.4. Heat Stress Analysis. Heat stress treatment was given at 45 ± 2°C. In the initial time points, a basal level of expression of 2.1 to 5.4-fold was maintained, and the peak of

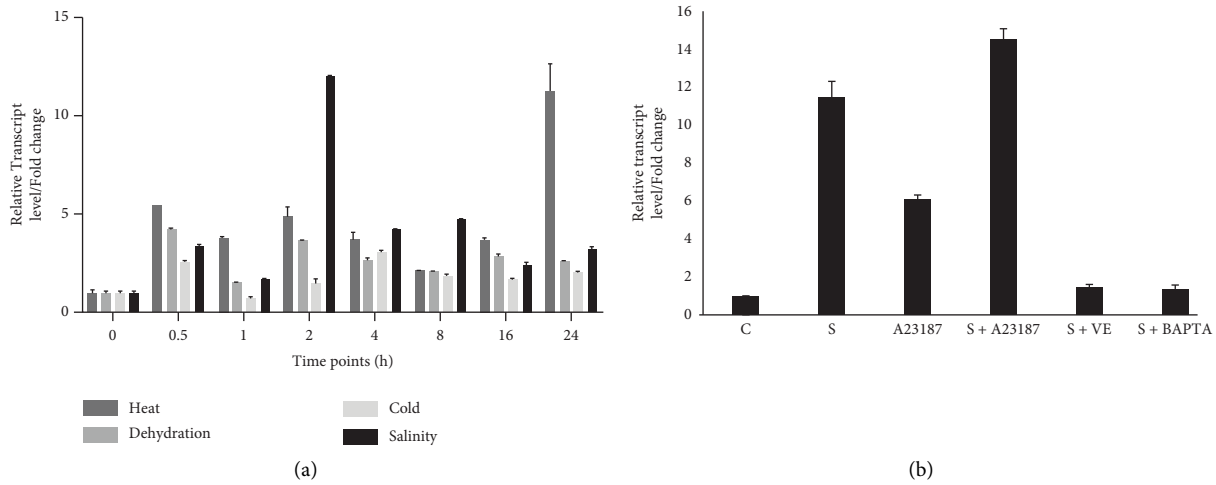

Figure 2: Expression analysis of *OsPAO3*. The expression analysis was performed from the *O. sativa* seedling/protoplast after the treatments. Extraction of RNA was conducted by RNeasy plant mini kit (Qiagen), followed by cDNA synthesis (high-capacity cDNA reverse transcription kit, Thermo Fisher Scientific). The cDNA obtained was used for expression analysis by real-time PCR using TaqMan probes. *OsPAO3* and *OseEF1* were labeled with the FAM MGB probe and VIC MGB probe (custom TaqMan™ gene expression assay), respectively. The assay was conducted by multiplexing. The assays were repeated with a minimum of three replicates, and ΔΔCT values were calculated; relative transcript level (fold change) was determined, and the graph was plotted. The *y*-axis shows the fold change while the *x*-axis in (a) shows the time points of abiotic stress treatment, and (b) shows various chemical treatments: C, control; S, sodium chloride (200 mM); A23187 (calcium ionophore, 50 μM); VE, verapamil (calcium channel blocker, 2 mM); and BAPTA, calcium chelator (2 mM). The data represent three biological replicates, and error bars have been shown.

expression of 11.2-fold was reached at 24 h of heat stress treatment (Figure 2(a)). In case of the heat stress, the peak of transcript accumulation was observed at late hours of treatment.

3.3. Calcium-Dependent Expression of OsPAO3. Furthermore, the probable involvement of calcium as a second messenger in the abiotic stress-induced PAO signal transduction was investigated. The studies were performed on protoplasts isolated from the 11-day-old *O. sativa* leaves. For calcium-related studies, the protoplast system was used, instead of seedlings due to the issue of permeability of specific chemicals used in the studies [25, 30, 31]. The protoplast obtained was treated with calcium channel ionophore A23187 (50 μM) [25, 26], calcium channel blocker verapamil [27], and calcium chelator BAPTA (1,2-bis(o-amino phenoxy) ethane-N,N,N′,N′-tetra acetic acid, 2 mM, [26, 28] in combination with abiotic stress. After the treatment, RNA extraction, cDNA synthesis, and real-time PCR analysis were performed as described earlier. Since the upregulation of *OsPAO3* transcript was the highest with respect to saline stress, hence for calcium-related studies, only saline stress was applied. The peak of *OsPAO3* transcript accumulation due to saline stress was observed at 2 h; hence, all the treatments were given for 2 h only. Calcium channel ionophore A23187 leads to the opening of calcium channels and the release of calcium from cellular storehouses [25, 26, 29], and verapamil is a calcium channel blocker that closes the calcium channel and does not allow the calcium to come out of the cellular storehouse [27], and BATPA is a calcium chelator which sequesters all the free calcium already present in the system [26, 28].

Upon treatment with calcium ionophore A23187, even in the absence of any kind of stress, the expression of *OsPAO3* was found to be increased to 6.1-fold (Figure 2(b)). Since A23187 leads to the opening of cellular calcium channels, suggesting that calcium might be involved in the expression of *OsPAO3*, when protoplasts were co-treated with ionophore A23187 and sodium chloride, the expression of *OsPAO3* further increased to 14.2-fold. The additive effect in expression suggested that ionophore A23187 and sodium chloride stress conditions both led to the release of calcium from the cellular storehouse, followed by an increase in the expression of *OsPAO3*. To further verify the involvement of calcium, the plant cells were treated with calcium channel blocker verapamil and calcium chelator BAPTA. The former obstructs the calcium channels, and hence, calcium was not able to release from the cellular storehouse despite the presence of stimuli, while the latter chelates all the free calcium in the cell. When the plant cells were treated either with verapamil or BAPTA in combination with sodium chloride, the expression level decreased drastically and remained comparable to untreated conditions (Figure 2(b)). This could be due to the fact that when sodium chloride treatment was provided either with a calcium channel blocker (verapamil) or calcium chelator (BAPTA), the stress treatment might have provided the signal for the release of calcium, but in the former scenario, the channels were blocked by the calcium channel blocker; hence, calcium was unable to come out of the cellular storehouse, while in the latter scenario, calcium was able to come out of cellular storehouse, followed by getting chelated due to the presence of calcium chelator; hence, the further downstream signaling could not take place, and *OsPAO3* expression did not occur. As per the data obtained, we suggest that upon the

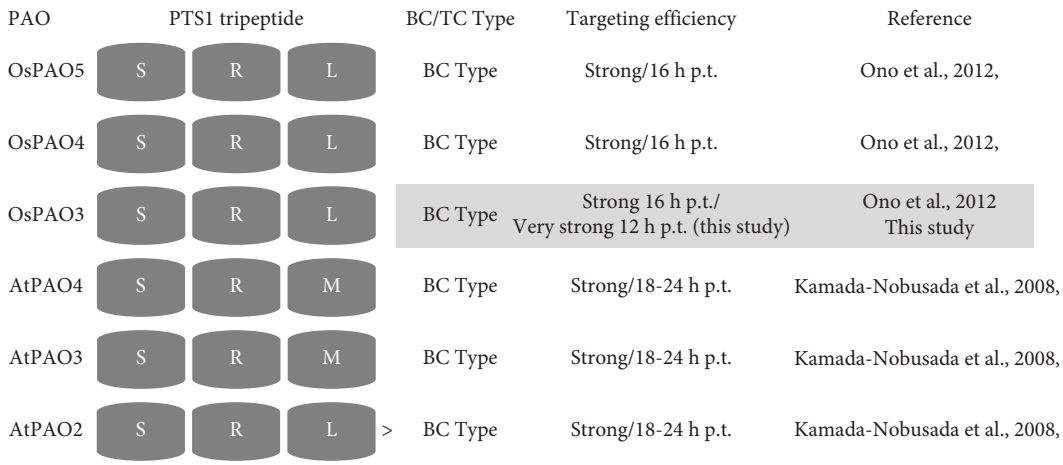

Figure 3: The figure shows the comparative information of *A. thaliana* and *O. sativa* peroxisomal PAOs. The grey boxes represent the PTS1 tripeptide. The greater sign (>) indicates the C-terminal end of the peptide. BC, back conversion; TC, terminal catabolism; p.t., post-transformation. The last column shows the literature reference. Except for OsPAO3, others have not yet been verified at 12 h p.t.

perception of stress conditions by plant cells, the stimuli led to an increase in the cellular concentration of the second messenger (calcium), which in turn led to the upregulation of *OsPAO3*.

4. Discussion

Polyamines have been known to play a major role in protecting the plant against environmental stresses [32]. The cellular homeostasis of PAs is largely controlled by PAOs [33], which are found in multiple subcellular locations: cytosol, cell wall, apoplastic regions, and peroxisomes [11, 34, 35]. Peroxisomes have been known to play a pivotal role in cellular ROS homeostasis [36]. In plant cells, the increase in the concentration of ROS is a common after-effect of abiotic stress conditions [32, 37]. If the accumulation of ROS is left unchecked, it may become detrimental to cells. Due to the considerable implication of PAOs and peroxisomes in abiotic stress-induced ROS homeostasis, the peroxisome-localized PAOs interest us particularly. In our studies, we have reported a PAO isoform 3 from *O. sativa* to be localized in the peroxisome within 12 h p.t. under *in vitro* conditions. The peroxisome localization of PAO has earlier been demonstrated; however, none of the previously reported peroxisomal PAOs were found to be targeted to the peroxisome as early as 12 h p.t. [4, 14], making OsPAO3 the only reported PAO targeted to the peroxisome within a very short span of time under *in vitro* studies, making it "early" peroxisome targeted PAO.

All the peroxisomal PAOs are targeted via peroxisome targeting signal (PTS) type 1, which is primarily represented by the last three amino acids, present at C-terminus [38]. The PTS1 signal in the case of OsPAO3, OsPAO4, and OsPAO5 was found to be SRL> (">" denotes the end of the polypeptide chain) in all three proteins, while the same in the case of AtPAO2, AtPAO3, and AtPAO4 is represented by SRL>, SRM>, and SRM>, respectively [4, 14] (Figure 3). The presence of two different types of PTS1s in *A. thaliana* suggests the occurrence of a greater diversity of PTS1 in *A. thaliana* as compared to *O. sativa*. Traditionally, depending upon the efficiency of PTS1, they have been categorized as canonical (strong) and noncanonical (weak). The classifications have been made on the basis of the time required for the reporter protein (fused with PTS1-containing protein) to be detected in peroxisomes under in vitro conditions [22, 39, 40]. The canonical PTS1 leads to "strong" targeting of reporter proteins and usually has a consensus sequence of (SA), (KR), and (LMI)> at −3, −2, and −1 positions, respectively. These largely do not depend upon the upstream residues. These have been found to occur frequently in the PTS1 proteins of higher plants and have been detected in peroxisomes within 18 h–24 h p.t. [22, 39, 40]. The noncanonical PTS1s require a comparatively longer time to be detected in the peroxisome. Usually, they are detectable in peroxisome 5–7 d p.t. The noncanonical ones are considered "weak" peroxisome-targeting signals [40]. However, recently, Skoulding et al. [41] further elaborated on the classification regarding the efficiency of PTS1s: very strong, strong, moderate, and weak. PTS1-carrying proteins fused to the reporter protein, leading to the detection of fluorescence in peroxisome within 12 and 18–24 h p.t., were categorized as very strong and strong, respectively, while proteins containing PTS1 requiring an extended time of 48 h and 5–7 d p.t. for the fluorescence to be detected in peroxisome have been referred as moderate and weak, respectively.

As per Skoulding et al. [41], SRM> has been demonstrated to be a very strong PTS1. In our studies, we reported OsPAO3 to be a very strong peroxisome targeting protein that contains SRL> as its PTS1, making SRL>, in addition to SRM>, another very strong PTS type 1. However, earlier targeting efficiency studies conducted by Skoulding et al. [41] have been performed on the last ten amino acids fused to a reporter protein, EYFP. This is a standard technique employed for the detection of peroxisomal protein [21, 39, 42–44]. Here, we have performed the localization studies using the full-length OsPAO3 protein fused to the reporter protein EYFP. We could detect OsPAO3 to be in

peroxisome 12 h p.t., suggesting it to be very strongly targeted. This is the first report of a full-length protein fused to EYFP to be detected in peroxisome 12 h p.t. and hence categorized as a very strong peroxisome-targeting signal containing protein.

All the peroxisomal PAOs have been reported to be BC-type. The BC-type PAOs lead to the back conversion of tetramine to triamines and triamines to diamines, thereby increasing the subcellular concentration of PAs, which help the plant in stress acclimation [45]. Furthermore, the expression pattern of *OsPAO3* was analysed in detail with respect to various abiotic stresses, namely, sodium chloride (salinity), cold, dehydration, and heat stress. It was found to be upregulated in the early time point (0.5–2 h) of stress treatment. Peroxisomal PAOs from *Citrus sinensis* and *Solanum lycopersicum* were also found to be upregulated by multiple abiotic stresses [10, 46]. Accumulation of higher levels of *OsPAO3* mRNA in earlier time points of abiotic stress treatment suggests that this particular peroxisomal PAO may have a defensive role in the early stages of stress acclimation and tolerance. This is further supported by the fact that OsPAO3 was found to be an early peroxisome targeting (12 h post-transformation) protein, as shown in Section 3.1. Furthermore, *OsPAO3* was found to be upregulated in case of sodium chloride, cold, dehydration, and heat stress, suggesting it to be a universal abiotic stress acclimation candidate. In the agricultural field, stresses do not act in isolation rather they work synchronously and in combinations. The extent of damage caused to standing crops by two or more abiotic stresses necessitates to the development of plants that are tolerant to multiple abiotic stresses. Agriculturally, important stress combinations, which usually impact the crops together and work synchronously, have been termed as "stress combination" [47] or "stress matrix" [48]. Salinity, dehydration, and cold stresses have been found to be acting synergistically against crop plants [48]. In the present study, *OsPAO3* mRNA was found to be accumulated to a higher extent in response to salinity, dehydration, and cold in earlier time points of treatment, suggesting that it could be a potential candidate for imparting tolerance against stress matrix/stress combination and for engineering plants against multiple abiotic stresses.

In plant cells, calcium has been known to act as a second messenger in a wide range of signal transduction pathways [16]. A transient increase in calcium has also been reported in response to abiotic stresses. The increase in cytosolic calcium concentration occurs due to calcium influx through the plasma membrane from extracellular sources and calcium release from intracellular stores [16]. In our studies, we could demonstrate that the expression of *OsPAO3* is mediated via second messenger calcium (Section 3.3). Previously, Monroy et al. [30] reported that the expression of cold acclimation-specific (cas) genes mediated by calcium using similar means. This would be the first report of its kind, where the involvement of calcium, as a second messenger, has been demonstrated in the PAO-mediated abiotic stress signal transduction network. However, previously, Ca^{2+} has been demonstrated to be linked with PA. In *A. thaliana*, Spd-dependent increase in cytosolic calcium has been demonstrated, [18] and an imbalance in calcium homeostasis in the absence of Spm resulting in hypersensitivity to saline stress has also been observed [49]. The export of PAs to apoplast leads to an influx of calcium, leading to an increase in cytosolic calcium concentration [50].

5. Conclusions

Polyamine oxidases have been reported to play a significant role in abiotic stress tolerance in plants [51]; however, the mechanism by which they impart tolerance remains elusive. It is believed that the BC-type PAOs lead to an increase in the cellular concentration of PA, thereby helping in abiotic stress acclimation. Incidentally, most of the BC-type PAO has been found to be peroxisomal in localization. Peroxisomes play a crucial role in cellular ROS homeostasis, which tends to get disrupted due to stress conditions. In this study, we have investigated a BC-type peroxisomal PAO from *O. sativa*, namely, OsPAO3. The OsPAO3 protein was detected in peroxisomes at 12 h p.t. under in vitro conditions, as demonstrated by fluorescent microscopy results. Hence, it was categorized as a very strong PTS1-containing protein meaning that it is an early peroxisome-targeting protein. The expression analysis of *OsPAO3* revealed that it was upregulated in the early time points of stress (salinity, dehydration, and cold) treatment. The early peroxisome targeting combined with the early upregulation of *OsPAO3* suggests that it could be instrumental in imparting abiotic stress acclimation to *O. sativa* plants at the initial stages of stress acclimation. In order to understand the signaling mechanism, we further studied the probable involvement of second messengers, and it was observed that calcium could be a probable second messenger in the PAO-mediated abiotic stress signal transduction. However, the performance of OsPAO3 further needs to be investigated in the *O. sativa* plants grown under field conditions where multiple abiotic stresses may be applied simultaneously to better understand the involvement of OsPAO3 in imparting tolerance against stress matrix or stress combinations. The stable transgenic *O. sativa lines*, overexpressing *OsPAO3* may also be generated.

Data Availability

The data (microscopic images and real-time PCR data) used to support the findings of this study are included within the article.

Conflicts of Interest

The authors declare that they have no conflicts of interest.

Authors' Contributions

GC conceptualized the idea, arranged for funding, and wrote the manuscript. IS and SC primarily performed the experiments. PCR helped with the microscopic image analysis.

Acknowledgments

The authors would like to thank the Scientific and Engineering Research Board (SERB), Department of Science and Technology (DST), Govt. of India, and School of Biotechnology, KIIT Deemed to be University, for the financial support for this research work.

References

[1] R. Alcázar, T. Altabella, F. Marco et al., "Polyamines: molecules with regulatory functions in plant abiotic stress tolerance," *Planta*, vol. 231, no. 6, pp. 1237–1249, 2010.

[2] M. D. Groppa, M. L. Tomaro, and M. P. Benavides, "Polyamines and heavy metal stress: the antioxidant behavior of spermine in cadmium- and copper-treated wheat leaves," *Biometals*, vol. 20, no. 2, pp. 185–195, 2007.

[3] Y. Takahashi, R. Cong, G. H. M. Sagor, M. Niitsu, T. Berberich, and T. Kusano, "Characterization of five polyamine oxidase isoforms in *Arabidopsis thaliana*," *Plant Cell Reports*, vol. 29, no. 9, pp. 955–965, 2010.

[4] Y. Ono, D. W. Kim, K. Watanabe et al., "Constitutively and highly expressed Oryza sativa polyamine oxidases localize in peroxisomes and catalyze polyamine back conversion," *Amino Acids*, vol. 42, no. 2-3, pp. 867–876, 2012.

[5] W. Wang, K. Paschalidis, J. C. Feng, J. Song, and J. H. Liu, "Polyamine catabolism in plants: a universal process with diverse functions," *Frontiers of Plant Science*, vol. 10, pp. 1–13, 2019.

[6] M. Cervelli, M. Bianchi, A. Cona et al., "Barley polyamine oxidase isoforms 1 and 2, a peculiar case of gene duplication," *FEBS Journal*, vol. 273, no. 17, pp. 3990–4002, 2006.

[7] T. M. Klein, E. D. Wolf, R. Wu, and J. C. Sanford, "High-velocity microprojectiles for delivering nucleic acids into living cells," *Nature*, vol. 327, no. 6117, pp. 70–73, 1987.

[8] M. Cervelli, O. D. Caro, A. D. Penta et al., "A novel C-terminal sequence from barley polyamine oxidase is a vacuolar sorting signal," *The Plant Journal*, vol. 40, no. 3, pp. 410–418, 2004.

[9] K. Yamaguchi-Shinozaki and K. Shinozaki, "Transcriptional regulatory networks in cellular responses and tolerance to dehydration and cold stresses," *Annual Review of Plant Biology*, vol. 57, no. 1, pp. 781–803, 2006.

[10] W. Wang and J. H. Liu, "Genome-wide identification and expression analysis of the polyamine oxidase gene family in sweet orange (Citrus sinensis)," *Gene*, vol. 555, no. 2, pp. 421–429, 2015.

[11] Z. Yu, D. Jia, and T. Liu, "Polyamine oxidases play various roles in plant development and abiotic stress tolerance," *Plants*, vol. 8, no. 6, p. 184, 2019.

[12] F. Gholizadeh and G. Mirzaghaderi, "Genome-wide analysis of the polyamine oxidase gene family in wheat (*Triticum aestivum* L.) reveals involvement in temperature stress response," *PLoS One*, vol. 15, no. 8, pp. 1–22, 2020.

[13] S. H. Habib, H. Kausar, and H. M. Saud, "Plant growth-promoting rhizobacteria enhance salinity stress tolerance in okra through ROS-scavenging enzymes," *BioMed Research International*, vol. 2016, Article ID 6284547, 10 pages, 2016.

[14] T. Kamada-Nobusada, M. Hayashi, M. Fukazawa, H. Sakakibara, and M. Nishimura, "A putative peroxisomal polyamine oxidase, AtPAO4, is involved in polyamine catabolism in *Arabidopsis thaliana*," *Plant and Cell Physiology*, vol. 49, no. 9, pp. 1272–1282, 2008.

[15] A. Raffaello, C. Mammucari, G. Gherardi, and R. Rizzuto, "Calcium at the center of cell signaling: interplay between endoplasmic reticulum, mitochondria, and lysosomes," *Trends in Biochemical Sciences*, vol. 41, no. 12, pp. 1035–1049, 2016.

[16] Y. Gao and G. Zhang, "A calcium sensor calcineurin B-like 9 negatively regulates cold tolerance via calcium signaling in *Arabidopsis thaliana*," *Plant Signaling & Behavior*, vol. 14, no. 3, pp. e1573099–6, 2019.

[17] R. Ozawa, C. M. Bertea, M. Foti et al., "Exogenous polyamines elicit herbivore-induced volatiles in lima bean leaves: involvement of calcium, H2O2 and jasmonic acid," *Plant and Cell Physiology*, vol. 50, no. 12, pp. 2183–2199, 2009.

[18] J. Wu, Z. Shang, J. Wu et al., "Spermidine oxidase-derived H2O2 regulates pollen plasma membrane hyperpolarization-activatedCa2+-permeable channels and pollen tube growth," *The Plant Journal*, vol. 63, no. 6, pp. 1042–1053, 2010.

[19] M. Fulda, J. Shockey, M. Werber, F. P. Wolter, and E. Heinz, "Two long-chainacyl-CoA synthetases from *Arabidopsis thaliana* involved in peroxisomal fatty acid β-oxidation," *The Plant Journal*, vol. 32, no. 1, pp. 93–103, 2002.

[20] P. Matre, C. Meyer, and C. Lillo, "Diversity in subcellular targeting of the PP2A B$'\eta$ subfamily members," *Planta*, vol. 230, no. 5, pp. 935–945, 2009.

[21] C. Ma, M. Haslbeck, L. Babujee, O. Jahn, and S. Reumann, "Identification and characterization of a stress-inducible and a constitutive small heat-shock protein targeted to the matrix of plant peroxisomes," *Plant Physiology (Bethesda)*, vol. 141, no. 1, pp. 47–60, 2006.

[22] G. Chowdhary, A. R. A. Kataya, T. Lingner, and S. Reumann, "Non-canonical peroxisome targeting signals: identification of novel PTS1 tripeptides and characterization of enhancer elements by computational permutation analysis," *BMC Plant Biology*, vol. 12, pp. 1–14, 2012.

[23] C. D'Onofrio and S. Lindberg, "Sodium induces simultaneous changes in cytosolic calcium and pH in salt-tolerant quince protoplasts," *Journal of Plant Physiology*, vol. 166, no. 16, pp. 1755–1763, 2009.

[24] I. Torrecilla, F. Leganés, I. Bonilla, and F. Fernández-Piñas, "Calcium transients in response to salinity and osmotic stress in the nitrogen-fixing cyanobacterium Anabaena sp. PCC7120, expressing cytosolic apoaequorin," *Plant, Cell and Environment*, vol. 24, no. 6, pp. 641–648, 2001.

[25] L. Qiu, Y. Wang, and H. Qu, "Loading calcium fluorescent probes into protoplasts to detect calcium in the flesh tissue cells of Malus domestica," *Horticultural Research*, vol. 7, no. 1, p. 91, 2020.

[26] K. De Vriese, A. Costa, T. Beeckman, and S. Vanneste, "Pharmacological strategies for manipulating plant Ca2+ signalling," *International Journal of Molecular Sciences*, vol. 19, no. 5, p. 1506, 2018.

[27] H. Knight, A. J. Trewavas, and M. R. Knight, "Calcium signalling in *Arabidopsis thaliana* responding to drought and salinity," *The Plant Journal*, vol. 12, no. 5, pp. 1067–1078, 1997.

[28] J. E. Dombrowski and D. R. Bergey, "Calcium ions enhance systemin activity and play an integral role in the wound response," *Plant Science*, vol. 172, no. 2, pp. 335–344, 2007.

[29] K. J. Livak and T. D. Schmittgen, "Analysis of relative gene expression data using real-time quantitative PCR and the $2-\Delta\Delta CT$ method," *Methods*, vol. 25, no. 4, pp. 402–408, 2001.

[30] A. F. Monroy, F. Sarhan, and R. S. Dhindsa, "Cold-induced changes in freezing tolerance, protein phosphorylation, and gene expression (evidence for a role of calcium)," *Plant Physiology (Rockville)*, vol. 102, no. 4, pp. 1227–1235, 1993.

[31] G. Gilliard, E. Huby, S. Cordelier, M. Ongena, S. Dhondt-Cordelier, and M. Deleu, "Protoplast: a valuable toolbox to

investigate plant stress perception and response," *Frontiers of Plant Science*, vol. 12, pp. 1–15, 2021.

[32] K. Gémes, Y. J. Kim, K. Y. Park et al., "An NADPH-oxidase/polyamine oxidase feedback loop controls oxidative burst under salinity," *Plant Physiology (Rockville)*, vol. 172, no. 3, pp. 1418–1431, 2016.

[33] R. Alcázar, F. Marco, J. C. Cuevas et al., "Involvement of polyamines in plant response to abiotic stress," *Biotechnology Letters*, vol. 28, no. 23, pp. 1867–1876, 2006.

[34] P. Fincato, P. N. Moschou, V. Spedaletti et al., "Functional diversity inside the Arabidopsis polyamine oxidase gene family," *Journal of Experimental Botany*, vol. 62, no. 3, pp. 1155–1168, 2011.

[35] P. Tavladoraki, A. Cona, and R. Angelini, "Copper-containing amine oxidases and FAD-dependent polyamine oxidases are key players in plant tissue differentiation and organ development," *Frontiers of Plant Science*, vol. 7, p. 824, 2016.

[36] L. M. Sandalio and M. C. Romero-Puertas, "Peroxisomes sense and respond to environmental cues by regulating ROS and RNS signalling networks," *Annals of Botany*, vol. 116, no. 4, pp. 475–485, 2015.

[37] K. A. Wilkins, E. Matthus, S. M. Swarbreck, and J. M. Davies, "Calcium-mediated abiotic stress signaling in roots," *Frontiers of Plant Science*, vol. 7, pp. 1–17, 2016.

[38] G. Neuberger, S. Maurer-Stroh, B. Eisenhaber, A. Hartig, and F. Eisenhaber, "Motif refinement of the peroxisomal targeting signal 1 and evaluation of taxon-specific differences," *Journal of Molecular Biology*, vol. 328, no. 3, pp. 567–579, 2003.

[39] T. Lingner, A. R. Kataya, G. E. Antonicelli et al., "Identification of novel plant peroxisomal targeting signals by a combination of machine learning methods and in vivo subcellular targeting analyses," *The Plant Cell*, vol. 23, no. 4, pp. 1556–1572, 2011.

[40] S. Reumann, G. Chowdhary, and T. Lingner, "Characterization, prediction and evolution of plant peroxisomal targeting signals type 1 (PTS1s)," *Biochimica et Biophysica Acta (BBA) - Molecular Cell Research*, vol. 1863, no. 5, pp. 790–803, 2016.

[41] N. S. Skoulding, G. Chowdhary, M. J. Deus, A. Baker, S. Reumann, and S. L. Warriner, "Experimental validation of plant peroxisomal targeting prediction algorithms by systematic comparison of in vivo import efficiency and in vitro PTS1 binding affinity," *Journal of Molecular Biology*, vol. 427, no. 5, pp. 1085–1101, 2015.

[42] J. Pessoa, Z. Sárkány, F. Ferreira-da-Silva et al., "Functional characterization of *Arabidopsis thaliana*transthyretin-like protein," *BMC Plant Biology*, vol. 10, no. 1, p. 30, 2010.

[43] C. Ma and S. Reumann, "Improved prediction of peroxisomal PTS1 proteins from genome sequences based on experimental subcellular targeting analyses as exemplified for protein kinases from Arabidopsis," *Journal of Experimental Botany*, vol. 59, no. 13, pp. 3767–3779, 2008.

[44] S. Reumann, L. Babujee, C. Ma et al., "Proteome analysis of Arabidopsis leaf peroxisomes reveals novel targeting peptides, metabolic pathways, and defense mechanisms," *The Plant Cell*, vol. 19, no. 10, pp. 3170–3193, 2007.

[45] P. N. Moschou, K. A. Paschalidis, I. D. Delis et al., "Spermidine exodus and oxidation in the apoplast induced by abiotic stress is responsible for H2O2 signatures that direct tolerance responses in tobacco," *The Plant Cell*, vol. 20, no. 6, pp. 1708–1724, 2008.

[46] Y. Hao, B. Huang, D. Jia et al., "Identification of seven polyamine oxidase genes in tomato (Solanum lycopersicum L.) and their expression profiles under physiological and various stress conditions," *Journal of Plant Physiology*, vol. 228, pp. 1–11, 2018.

[47] S. I. Zandalinas, F. B. Fritschi, and R. Mittler, "Signal transduction networks during stress combination," *Journal of Experimental Botany*, vol. 71, no. 5, pp. 1734–1741, 2020.

[48] R. Mittler, "Abiotic stress, the field environment and stress combination," *Trends in Plant Science*, vol. 11, no. 1, pp. 15–19, 2006.

[49] K. Yamaguchi, Y. Takahashi, T. Berberich et al., "The polyamine spermine protects against high salt stress in *Arabidopsis thaliana*," *FEBS Letters*, vol. 580, no. 30, pp. 6783–6788, 2006.

[50] I. Pottosin and S. Shabala, "Polyamines control of cation transport across plant membranes: implications for ion homeostasis and abiotic stress signaling," *Frontiers of Plant Science*, vol. 5, pp. 1–16, 2014.

[51] D. Chen, Q. Shao, L. Yin, A. Younis, and B. Zheng, "Polyamine function in plants: metabolism, regulation on development, and roles in abiotic stress responses," *Frontiers of Plant Science*, vol. 9, pp. 1–13, 2018.